## Does Quantum Interference Control of injected Photocurrents Produce a Current or Voltage?

Yiming Gong, Steven. T. Cundiff

Physics Department, University of Michigan, Ann Arbor, Michigan, 48109, USA ymgong@umich.edu, cundiff@umich.edu

**Abstract:** We address the question "Does Quantum Interference Control (QuIC) of injected Photocurrents Produces a Current or Voltage?" by studying the dependence on external resistance for Schottky- and Ohmic- contact devices, resolving a long-standing puzzle. © 2024 The Author(s)

Quantum Interference Control (QuIC) manipulates a system through the interference of two independent pathways coupling the same initial and final states. The interference, contributing constructively or destructively to the transition amplitude [1], is effectively a "matter interferometer," where the laser phase is a key control parameter. It has been explored in different systems such as atomic gases, molecular systems, and semiconductors. In 1997, Haché et al. [1] experimentally observed the first QuIC of current in GaAs using electrodes to collect the accumulated charge displacement. The QuIC injected photocurrent is a sine function of the relative phase between two optical absorption pathways. To our best knowledge, the semiconductor devices in the previous studies [2] of QuIC all have Schottky barriers at the semiconductor-metal interfaces, which makes the carrier transport through the interface nontrivial. The Schottky barriers give rectifying properties to the device due to the difference in electronic affinity between the metal and the semiconductor. The carriers injected by QuIC processes accumulate underneath the metallic electrodes instead of tunneling through the interface, which makes the metal-semiconductor-metal (MSM) structure effectively a capacitor. The capacitor provides a voltage across the semiconductor and external circuit. However, theoretically the direct product of OuIC should be a net current flowing out of the device. This introduces the puzzle of does QuIC of injected photocurrents produce a current or voltage. We address this puzzle by studying the external resistance dependence of the photocurrent injected by QuIC of one- and two- photon absorptions (1+2 QuIC).

## 1+2 QuIC Experiment

Second Harmonic Generation in a 100  $\mu m$  BBO crystal doubles the frequency of an optical frequency comb, which is centered at 1040 nm. The repetition rate of the comb is 250.583 MHz. A prism pair separates the 1040 nm light from its second harmonic spatially. The spacing between the two prisms is about 40 cm. The 520-nm arm of the interferometer was dithered sinusoidally over about  $\lambda/4$  at 2 KHz for lock-in detection. The 1040-nm arm was ramped sinusoidally over several wavelengths at 0.5 Hz. The two driving voltages of piezos are phase-stable relative to the same DDS clock. The diameter of the focal spot of the 1040-nm beam is  $\sim 2~\mu m$ , and the diameter of the focal spot of the 520 nm beam is  $\sim 3~\mu m$ . The power of 1040-nm illumination is  $\sim 42~mW$ , and the power of 520 nm illumination is  $\sim 8~mW$ . The 1+2 QuIC current is converted to a voltage signal by an external resistance, which is the load resistor of the voltage channel of the Lock-in Amplifier (10M $\Omega$ ) and Decade Box (0-10M $\Omega$ ) in parallel.

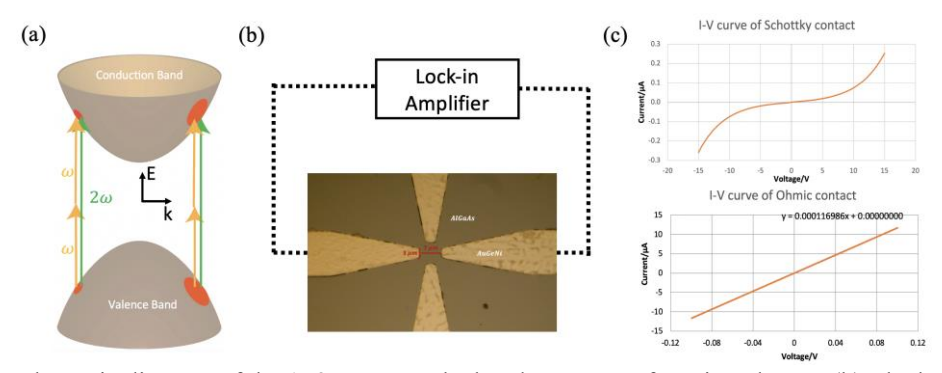


Figure 1. (a) A schematic diagram of the 1+2 QuIC on the band structure of semiconductor. (b) The horizontal electrode pair connects to a Lock-in Amplifier. The Schottky and Ohmic devices have the same electrode pattern. (c) Top: the I-V curve of the Schottky device. Bottom: the I-V curve of the Ohmic device.

We use one AlGaAs device with Schottky barrier and another AlGaAs device with Ohmic contact as the QuIC photocurrent sources. The two devices have the same electrode pattern, which is shown in Fig. 1 (b). The 1040 nm light and its second harmonic are both linearly polarized across the horizontal electrode pair. A Lock-in Amplifier in Voltage mode detects the current from the horizontal electrode pair at the fast dither frequency. The I-V curves of these two devices are shown in Fig. 1 (c). The Schottky device has a much larger effective resistance ( $\sim 100 \text{ M}\Omega$ ) than the Ohmic device ( $\sim 8.5 \text{ K}\Omega$ ).

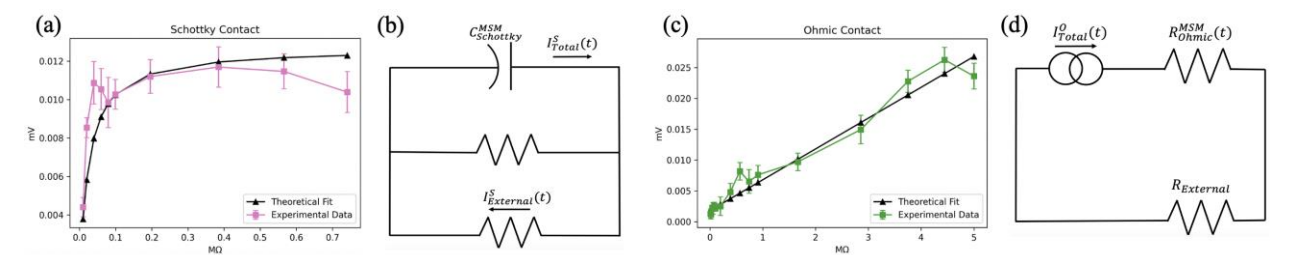


Figure 2. In the measurement of 1+2 QuIC in Schottky device, the pink solid line in (a) denotes the amplitude of QuIC signal as a function of the external resistance. The variance of each data point is indicated by the error bars. The solid black line denotes the theoretical fit of the data based on the circuit model in (b). In the measurement of 1+2 QuIC in Ohmic device, the green solid line in (c) denotes the amplitude of QuIC signal as a function of the external resistance. The variance of each data point is indicated by the error bars. The solid black line denotes the theoretical fit of the data based on the circuit model in (d).

For the Schottky contact sample, the metal-semiconductor-metal structure is modeled by a capacitor and a resistor in parallel. The capacitor is discharged periodically in time, which creates the current flow in the external circuit. The circuit and the external circuit are two discharging channels of the capacitor. The capacitance is denoted by  $C_{Schottky}^{MSM}$ . The resistances of the Schottky device and Ohmic device are denoted by  $R_{Schottky}^{MSM}(t)$  and  $R_{Ohmic}^{MSM}(t)$ , respectively. We also have  $I_{Total}(t) = I_{Total}(t+T)$ , where T is the time interval between pulses. We assume that the injected current  $\langle I_{Total}^{S}(t) \rangle$  roughly remains constant under the change of  $R_{External}$  in the low external resistance regime, where  $I_{Total}^{S}(t)$  is split into  $R_{Schottky}^{MSM}(t)$  and  $R_{External}$ . The voltage measured by Lock-in Amplifier from the Schottky-contact sample can be written as a function of external resistance:  $V_{Schottky}$ 

 $\frac{\langle l_{Total}^{S}(t) \rangle R_{External} \langle R_{Schottky}^{MSM}(t) \rangle}{R_{External} + \langle R_{Schottky}^{MSM}(t) \rangle}.$  The external resistance dependence was fitted by this function, as shown in Fig. 2 (a).

The fitted  $\langle R_{Schottky}^{MSM}(t) \rangle$  and  $\langle I_{Total}^{S}(t) \rangle$  are 23.5  $K\Omega$  and 5.4×  $10^{-7}A$ , respectively. The discrepancy between  $\langle R_{Schottky}^{MSM}(t) \rangle$  and the resistance of Schottky device under illumination (( $\sim 37 \text{ K}\Omega$ ) is possibly due to the recovery of high effective resistance after each pulse. As the external resistance increases, the charges transfer across the depletion layer to the metal-semiconductor interface become more saturated. Therefore, the voltage plateaus in the high external resistance regime, possibly because there are not enough charges yielding an increasing voltage. These features of the Schottky MSM device make exhibit a "voltage source" that provides roughly constant voltage for a wide range of external resistance. Different from Schottky contact, the capacitance of Ohmic contact is mostly parasitic and much lower. The charges transfer across the depletion layer through the tunneling process instead of thermionic emission. Therefore, we use the circuit in Fig. 2 (b) as our model, where the device provides the injected carriers as a current source. In the high external resistance regime, the voltage across the external resistor can be fitted by a linear function:  $V_{Ohmic} = \langle I_{Total}^o(t) \rangle R_{External} + V_0$ . The fitted parameters  $\langle I_{Total}^o(t) \rangle$  and  $V_0$  are  $5 \times 10^{-9} A$  and 0.0018 mV, respectively. As shown in Fig. 3.11, the linear trendline and the resistance dependence show a fairly good agreement.  $\langle I_{Total}^o(t) \rangle$  is much smaller than  $\langle I_{Total}^s(t) \rangle$ , possibly because the voltage also plateaus to some degree due to the charge transfer saturation. In summary, the Schottky contact QuIC device external-resistance dependence exhibits the voltage-source feature, while the Ohmic contact QuIC device external-resistance dependence exhibits the current-source feature.

## References

- [1] A Haché et al. "Observation of coherently controlled photocurrent in unbiased, bulk GaAs". In: Physical Review Letters 78.2 (1997), p. 306.
- [2] Alain Haché. "Coherent control of photocurrent in bulk semiconductors". PhD thesis. 1998.